Configuration Design of Smart Structures with Array Antennas

Minsung Kim
The 7th (Aircraft Systems) R&D Institute, Agency for Defense Development
Principal Researcher
Youseong-gu, P.O. Box 35-7, Daejeon 305-600, Republic of Korea
castle@add.re.kr

Sangmin Baek
The 7th (Aircraft Systems) R&D Institute, Agency for Defense Development
Researcher

Myunggyun Ko
The 7th (Aircraft Systems) R&D Institute, Agency for Defense Development
Researcher

Jongwoo Seo
The 2nd (Command/Control/Information) R&D Institute, Agency for Defense Development
Senior Researcher

Youngsik Joo
The 7th (Aircraft Systems) R&D Institute, Agency for Defense Development
Principal Researcher

ABSTRACT

This study proposes a new configuration design of conformal load-bearing array antenna structures (CLAAS). The CLAAS, when delployed as the upper skin of and aircraft fuselage, can bear aerodynamic loads. The configuration design considers structural and antennal requirements. The maximum allowable deflection is one of these requirements. The simulation results shows that the CLAAS deflects 0.5% of one edge length in the out-of-plane direction. The array antenna should perform within the maximum deflection range although the deflection shape differs depending on the structural load conditions. This study presents the antenna performance results for several deflection shapes. A Ku-band array antenna was embedded in the CLAAS. Tile antennas should operate without performance reduction under those deflected configuration. The deflected shape and deflection size were verified with structural tests. The antenna comprised 64 tile antennas in and 8×8 rectangle array configuration. Each tile has 64 radiating elements that act as a single antenna unit.

KEYWORDS: *Conformal Load-bearing Array Antenna Structure (CLAAS); Smart Skin; Array Antenna; Grid Structure*

NOMENCLATURE

Abstract text formatting: Font:
θ_c – slope of y-direction
θ_t – minimum slope of y-direction
R – radius of curvature
Tx – tile width
R_m – tile position from observation point
r_m – tile position from origin
$\hat{p}$ – position transition vector
E – Electric Field
a_n – complex weighting
P – element pattern
α_m- constant
β_m- electric field index
D_m- Relative Delay
W_{LTD_float} – floating control number in long time delay (LTD)
W_{LTD_fixed} – fixed control word in LTD
W_{STD_float} – floating control number in LTD
W_{STD_float} – fixed control word in LTD

1 INTRODUCTION

The conformal antenna has important advantages as a replacement for a blade antenna or a reflector antenna. Its aerodynamic efficiency gives it good fuel efficiency and a wider usage range. In particular, it gives a low radar cross section (RCS) when applied to military aircraft [1], as depicted in Fig. 1. To install a conformal antenna in an aircraft, the location should be studied considering antenna performance, airframe configuration, EMI/lightning protection, and maintenance [2]. The aircraft skin structure can bear aerodynamic loads, and it deflects when an aerodynamic load is applied. The conformal antenna should operate under the maximum deflection of the installed position. Harmen *et al.* [3] predicted the distortional deflection that occurs when a conformal antenna is installed on the reconnaissance pod skin of fighter-type aircraft.

This paper proposes a new configuration design of conformal load-bearing array antenna structures (CLAAS). The CLAAS is known as an essential technology for the design of a stealth aircraft because it reduces the RCS. The CLAAS also reduces aerodynamic drag, so that the aircraft operates with good fuel efficiency. Reconnaissance aircraft of unmanned air vehicles (UAVs) have many antennas and radars. The antenna usage determines the antenna frequency, size, configuration, etc. The aim of CLAAS development is to verify its load capability and antenna performance together.

The CLAAS can bear the aerodynamic loads, and it deflects when it bears such loads. Unfortunately, antenna performance is sensitive to the structural deflection. From the antenna's perspective, the deflection of the structures should be minimized. The CLAAS is designed as the upper skin of the UAV center fuselage considering antenna's best performance during the operating maneuver. Among numerous structural load conditions of aircraft design loads, a few critical load conditions are selected to size the CLAAS structures. The deflection shape and deflection length are derived according to the structural analysis results for the selected load conditions.

The antenna system in the CLAAS is a tile-based array antenna for receiving communication signals from the satellite. The smallest antenna unit is the radiating element. A tile has 64(8×8) radiating elements and a cell is made of 16(4×4) radiating elements. The antenna system comprises 64(8×8) tiles. Electromagnetic performance is calculated for the tile antenna. The CLAAS antenna system has a broad-band broad-angle beam steering angles and has a performance that is equivalent to that of the reflector-type antenna system.

From the aforementioned CLAAS, structures and the antenna are fabricated together to bear aerodynamic loads. Antenna performance is analyzed for the deflected structural shape to check the maximum allowable deflection as a design parameter. The deflection can occur in the x-, y-, z-directions, but this study deals with out-of-plane deflection, i.e., z-directional deflection, because it is dominant in comparison with x-, and y-directional deflections. Each tile antenna is attached to the bottom of the housing structure. Thus, the out-of-plane deflection of each tile location center is measured when the load is applied. MATLAB code is used to simulate the electromagnetic performance of the deflected antenna system. The active return loss and gain are derived as the simulation results.

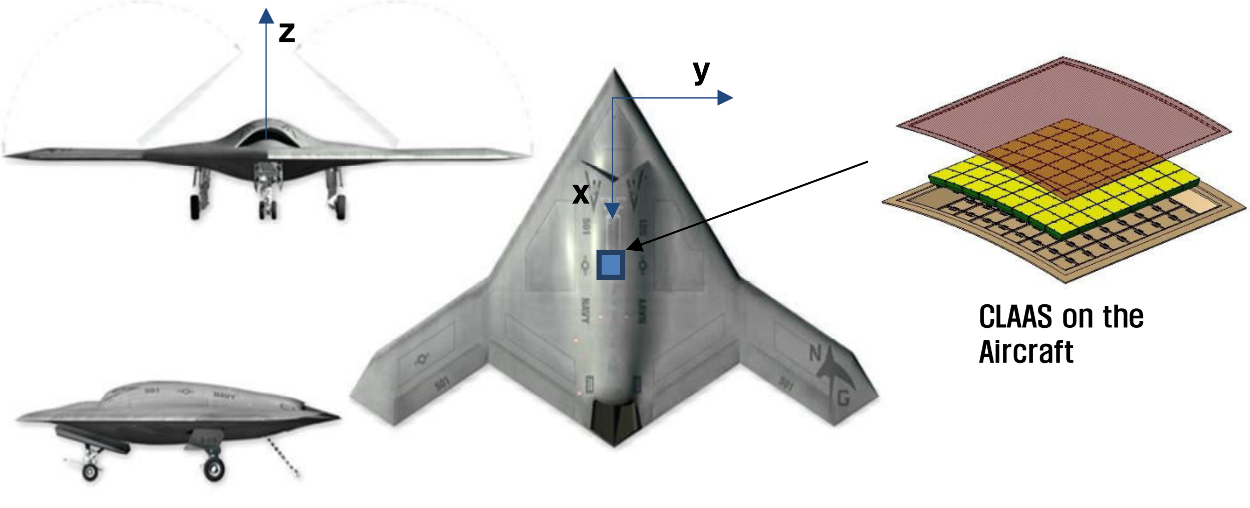

Figure 1: CLAAS installed on the UAV r[1].

2 CLAAS DESIGN

2.1 Design Object

The structural and antennal design requirements for designing the CLAAS configuration are described in Table 1. Structural design objectives are that the CLAAS structure should have optimum weight and size with enough stiffness and strength within the range of full antennal performance. It is assumed that the CLAAS is located on the back skin of the fuselage made of CFRP composite materials. As many as 242 load conditions are used to design the configuration of the back skin, and six load conditions were selected to represent other load conditions. The tile antennas are located on the bottom of the housing plate. The housing plate should provide enough stiffness to the tile antennas so that the antenna system performs during the flight operation without signal disconnection.

Table 1: CLAAS Design Requirements

Requirements	Value	Description
Impact strength	4 ft-lb	No visual damage
Allowable deflection	x %	Out of plane(long edge length)
Stiffened structure	Grid structure	Ortho-grid
Housing plate	Curved surface	One-directional curve
Buckling strength	No buckling	For load conditions
Antenna angle	60°	Broad angle

2.2 Material Properties

The material properties of the CLAAS are decided based on the applied platform materials. The material of aircraft skin and frames is generally made of CFRP composite. The Cycom CFRP material was also selected as the housing plate as shown in Table 2. The material with best electromagnetic properties was selected for the radome face-sheet of the antenna. Glass/epoxy, aramid/benzoxazine and quartz/cyanate ester were the candidates for radome materials. Quartz/cyanate ester has lower electromagnetic properties comparing with glass/epoxy and has better structural strength compared with aramid/benzoxazine. Therefore, quartz/cyanate ester is chosen as the radome skin material. Radome is designed as an A-sandwich type structure which is composed of a core and a face-sheet, ROHA-CELL is selected as the core material because of its general characteristics and high glass transition temperature. The material properties of CFRP and face-sheet are derived from in-house test results and the values of core are derived from data-sheets from the supplier of ROHA-CELL 51WF.

Table 2: CLAAS Material Properties

Properties	E_{11} (GPa)	F_{tu} (MPa)	ν_{12}	G_{12} (GPa)
CFRP(housing)	64.02	823	0.06	3.65
Radome face-sheet	23.1	558	0.13	4.07
Radome core	0.075	1.6	0.5	0.024

2.3 Housing Structure

Fig. 1 shows the concept diagram that CLAAS is installed on the aircraft fuselage skin. CLAAS has a planar shape to x-direction and circular shape to y-direction because it is simulated to locate on the back skin of a reconnaissance aircraft. Housing structures are made of carbon fiber reinforced polymers and composed of a frame structure and bottom plate with 1000x1000 mm size. The antenna system is consisted of 64 antenna tiles and each tile is attached to the bottom plate by screws. The tile antenna has 64 minimum antenna units called radiating elements. One tile is the standard antenna for CLAAS system development. Tiles are arrayed with different shapes just like diamond and circle, but rectangle shape is finally chosen to reduce the size of the array antenna system. Because tile has a rectangular shape, rectangle housing plate shape is the optimum configuration to reduce the size of the array antenna system. Frame of housing structure is the main load path where aerodynamic load carries. The grids of the housing structure are placed to support additional stiffness of housing plate and indicate the location of antenna tiles. The grids has 5 mm width and 4 mm height. The grids are stacked and fabricated together with bottom plates. The gaps between tile antennas are the same 1 mm for both x and y-axis direction after attached to the bottom plate.

2.4 Radome

The conformal load-bearing array antenna made of radome, antenna and housing structures are shown in Fig. 2. Radome is made of glass fabric composites called quartz/cyanate ester and ROHA-CELL. Radome has an A-sandwich configuration. Quartz/cyanate ester has a good dielectric constant and loss tangent compared with other glass fabric materials, as summarized in Table 3. The thickness of the face-sheet and core cell is decided after structural and electromagnetic analysis. Static analysis, buckling analysis, and normal mode analysis were conducted for a single core of 4mm thickness and two face-sheets each of 1.25 mm thickness. The total thickness of radome is 6.5 mm.

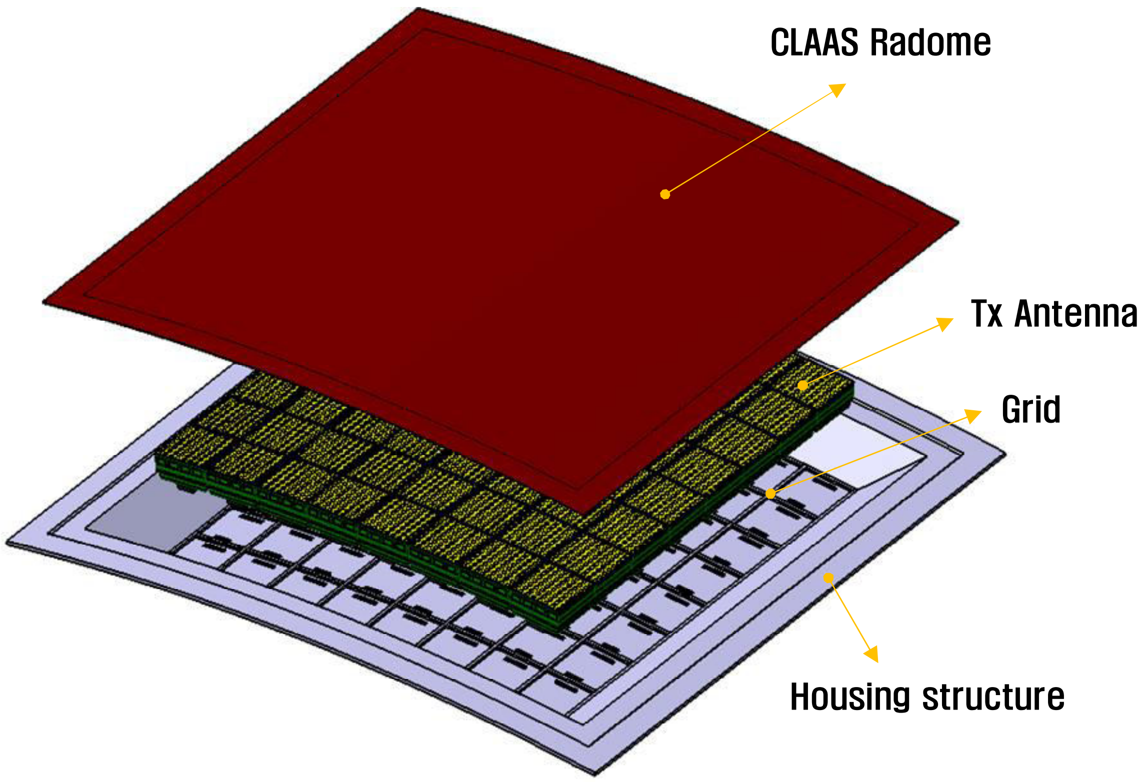

Figure 2: The configuration of the CLAAS.

Table 3: Radome Material

Material	Modulus (GPa)	Shear modulus (GPa)	Poisson's ratio	Dielectric constant Dk(10GHz)	Loss tangent Df(10GHz)
Quartz/cyanate ester	23.1	4.07	0.13	3.1	0.007
Glass/epoxy	23.2	4.1	0.14	4.062	0.0173
Aramid/benzoxazine	29.7			2.351	0.0124

3 CLAAS DEFLECTION

The CLAAS deflects when an aerodynamic load is applied. The deflection of the bottom plates affects the antenna performance. To predict the structural deformation, the finite elements of the CLAAS are modeled by HYPERMESH software(s/w), which is well known for its powerful automatic mesh generation, high fidelity, and direct interfacing with the CATIA s/w design model. There are many connector holes in the housing structure of the CLAAS, and HYPERMESH is applied to generate meshes near the connector holes efficiently with the geometric clean-up function. The housing and radome are modeled by two-dimensional shell elements such as CQUAD4 and CTRIA3, the grid is modeled by three-dimensional solid elements (CHEXA), and bolts is modeled by one-dimensional bar elements (RBE2). The number of elements is 55,628. The worst element aspect ratio and skew angle are 1.9 and 62°. Structural analysis was conducted with NASTRAN s/w which is a famous structural analysis program that has been used to perform static, dynamic, and thermal analysis across the linear and nonlinear domains in the aerospace world since 1960.

3.1 Structural Analysis

The static load analyses were conducted to derive the deflected shape for several load conditions as described in Table 4. Tension/compressions in the x- and y-axis directions, shear in the xy-axis direction, and bending in the z-axis direction are considered in the load conditions. Fig. 3 shows boundary conditions for LC 1 to LC 7. Fig. 4 to Fig. 6 show three worst cases among the static load analysis results. A two-dimensional shell element was applied for the housing and radome and a three-dimensional solid element was applied to the grid structure in the finite element model (FEM). The antenna configuration is not included in the FEM. The weight of each tile, 300g, is considered in the inertia load analysis and normal mode analysis. Fig. 4 shows the deformed shape of the CLAAS for load case 3 with a scale factor 50. Radome deforms 4.03 mm in the z-axis direction, and the housing deforms 1.87 mm in the z-axis direction separately. The deflection shapes for load cases 5, and 6 also show deflections of radome and housing with different configurations in Figs. 5 and 6.

Table 4: Load Case

Load case	Description	Load	Notes
LC1	Tension x-direction	500 $\mu\varepsilon$	Nominal strain
LC2	Compression x-direction	-500 $\mu\varepsilon$	Nominal strain
LC3	Tension y-direction	700 $\mu\varepsilon$	Nominal strain
LC4	Compression y-direction	-700 $\mu\varepsilon$	Nominal strain
LC5	Shear xy-direction	500 $\mu\varepsilon$	Nominal strain
LC6	Bending x-direction	10 mm	Out-of-plane displacement
LC7	Bending y-direction	10 mm	Out-of-plane displacement

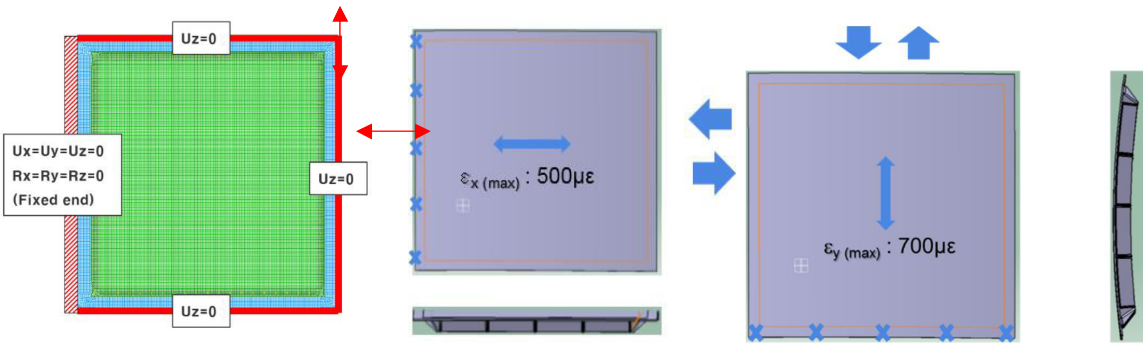

Boundary conditions for LC1 to LC4

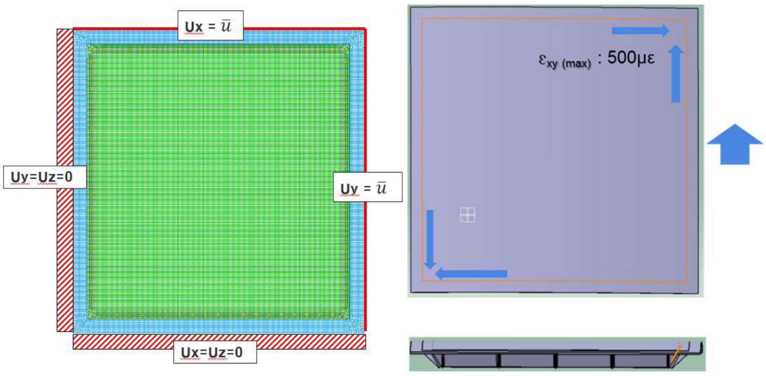

Boundary conditions for LC5

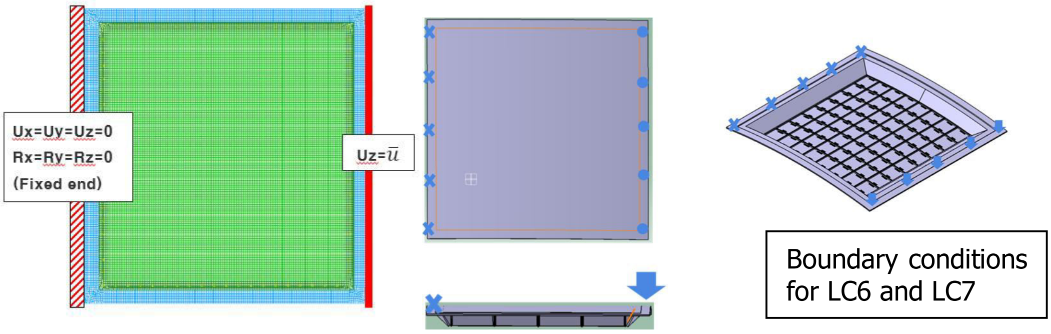

Figure 3: Boundary conditions for LC1 to LC7.

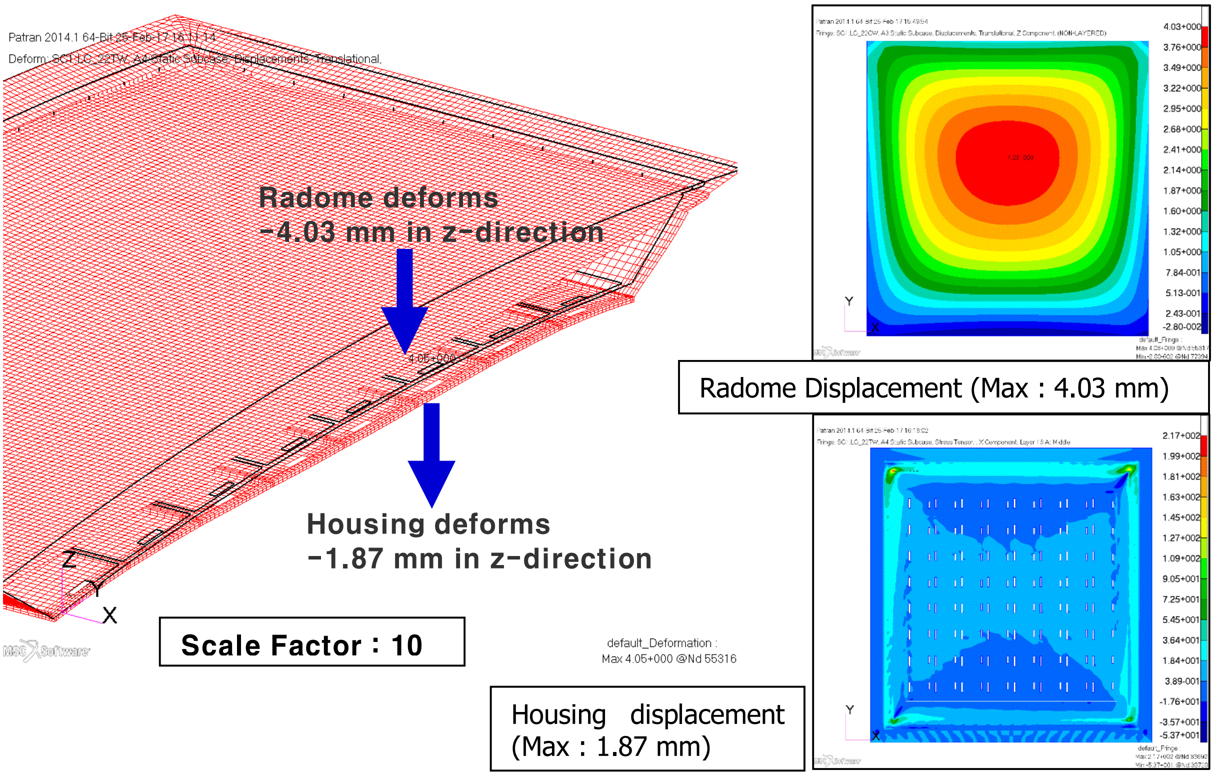

Figure 4: Deflection shape and displacement contour for LC3.

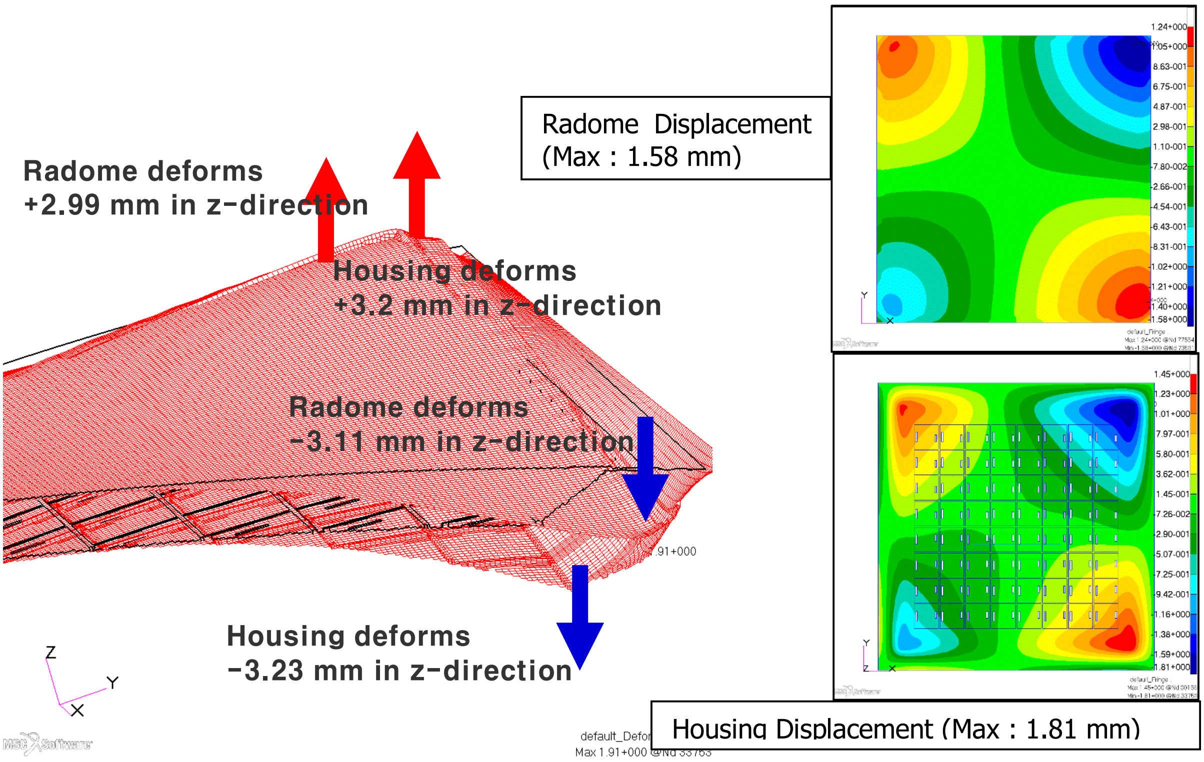

Figure 5: Deflection shape and displacement contour for LC5.

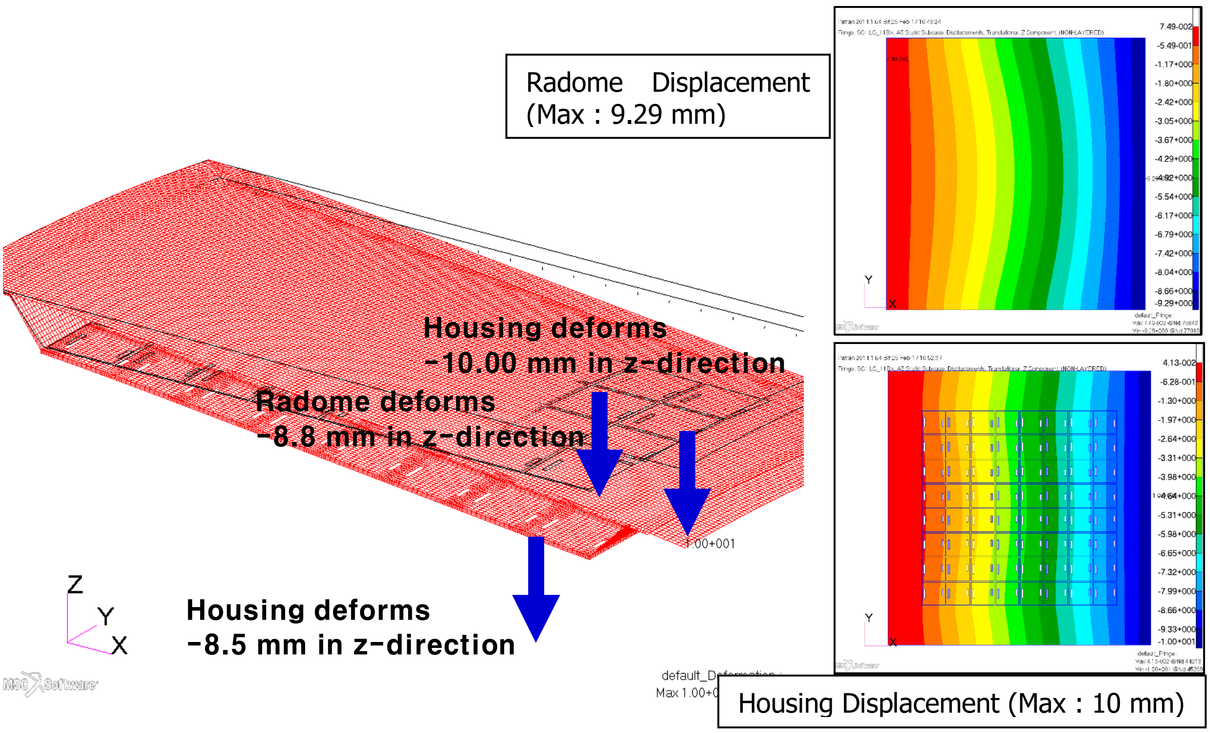

Figure 6: Deflection shape and displacement contour for LC6.

Stress contours and strength calculation results are shown in Fig. 7. The stress contours of LC 5 in the x-, y-, and xy- directions for radome and housing are presented separately to show the integrity of the FEM, as shown in Fig. 7.

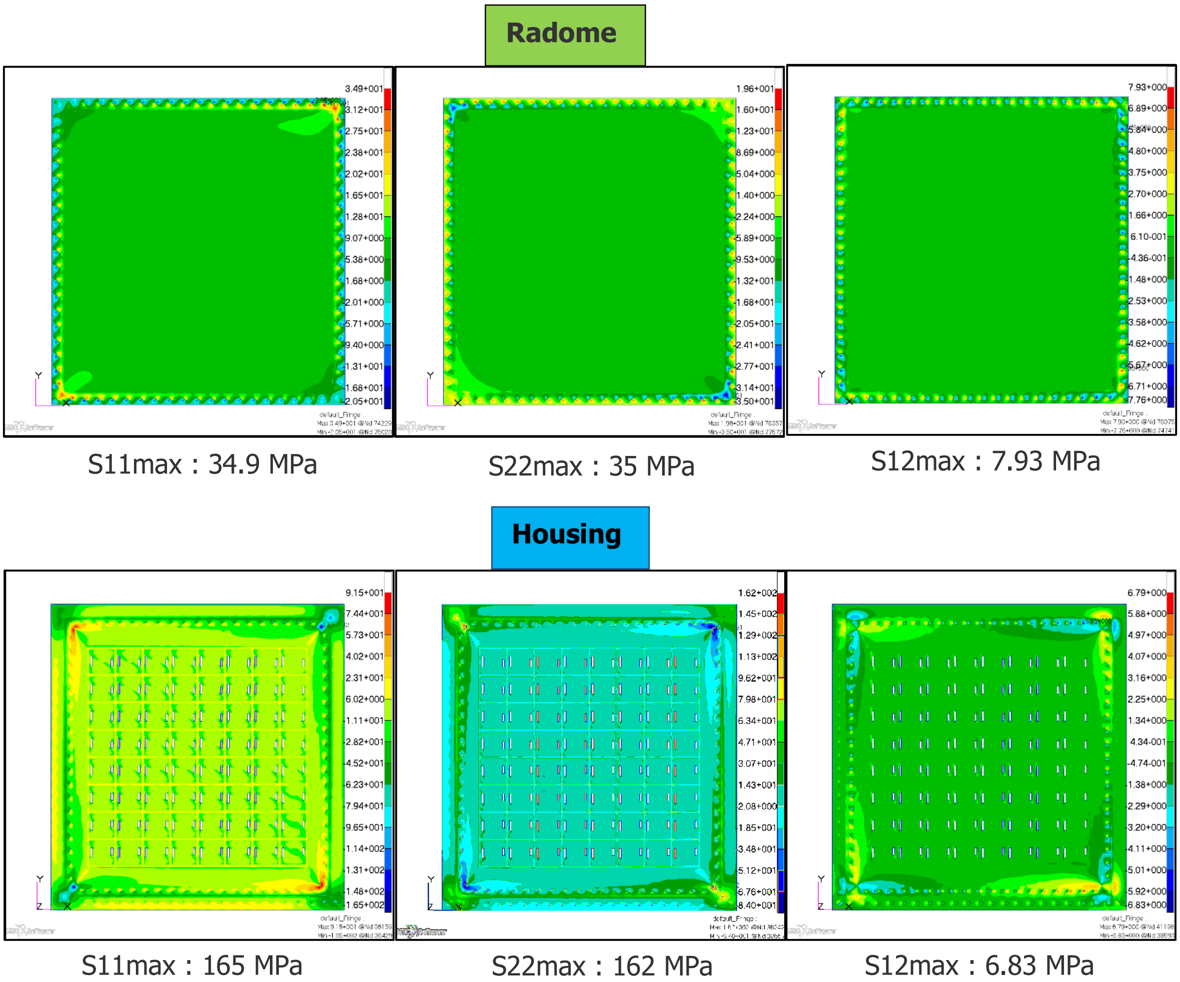

Figure 7: Stress contour of CLAAS for LC 5.

3.2 Conformal Array Analysis

Planar tile antennas are placed on a cylindrical surface in the y-direction on the aircraft. The radome, tile antennas, and housing plate in the y-direction are shown in Fig. 8. Tx is the tile size, and θ_c is the slope of the y-direction of a planar tile on the cylindrical surface. R is the radius of curvature, i.e., 3500 mm. To calculate the control bit for coherent phase summation considering these slopes per tile, the relative delay equation is derived in Fig. 8. The floating control number, word, and LTD control error are considered in the conformal array analysis. The array factor is derived on the basis of the cylindrical coordinate system, as shown in Fig. 8. The cylindrical tile array is located on the sphere surface as shown in Fig. 9. Each tile has a slope of θ_c, and a minimum $\theta_c = \theta_t$ is assumed to prevent overlap of two cylindrical tile arrays.

(a) Radome, tiles, and housing plate on the curved surface.

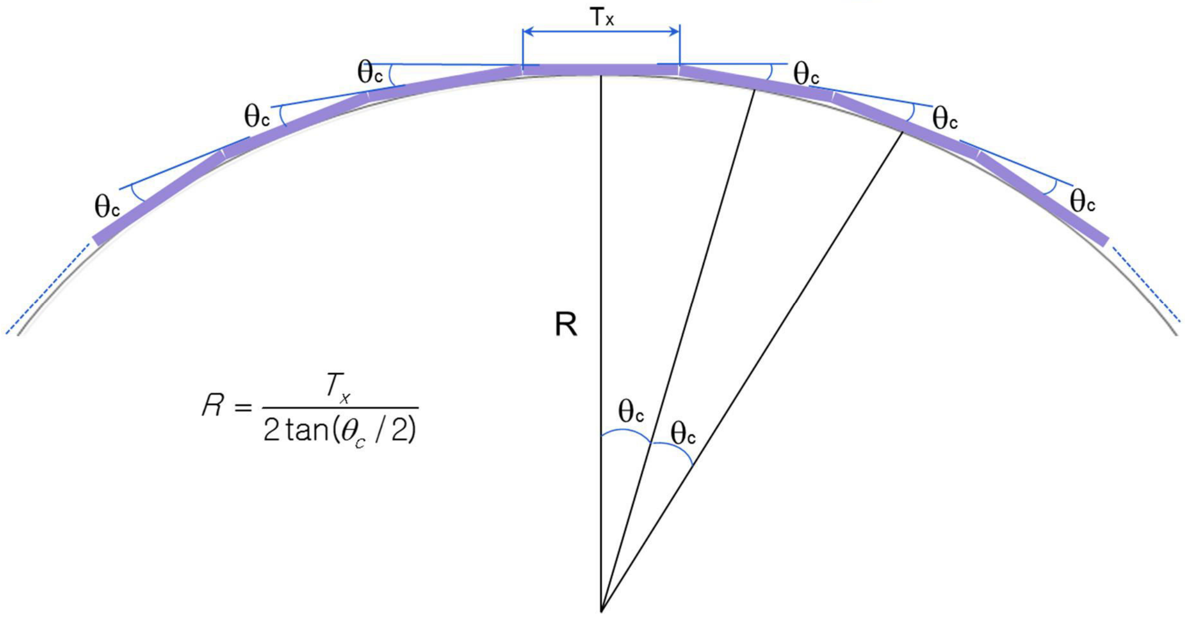

(b) Slopes of tile antenna with Tx length

Figure 8: Placement of planar tiles on cylindrical surface with scale-up.

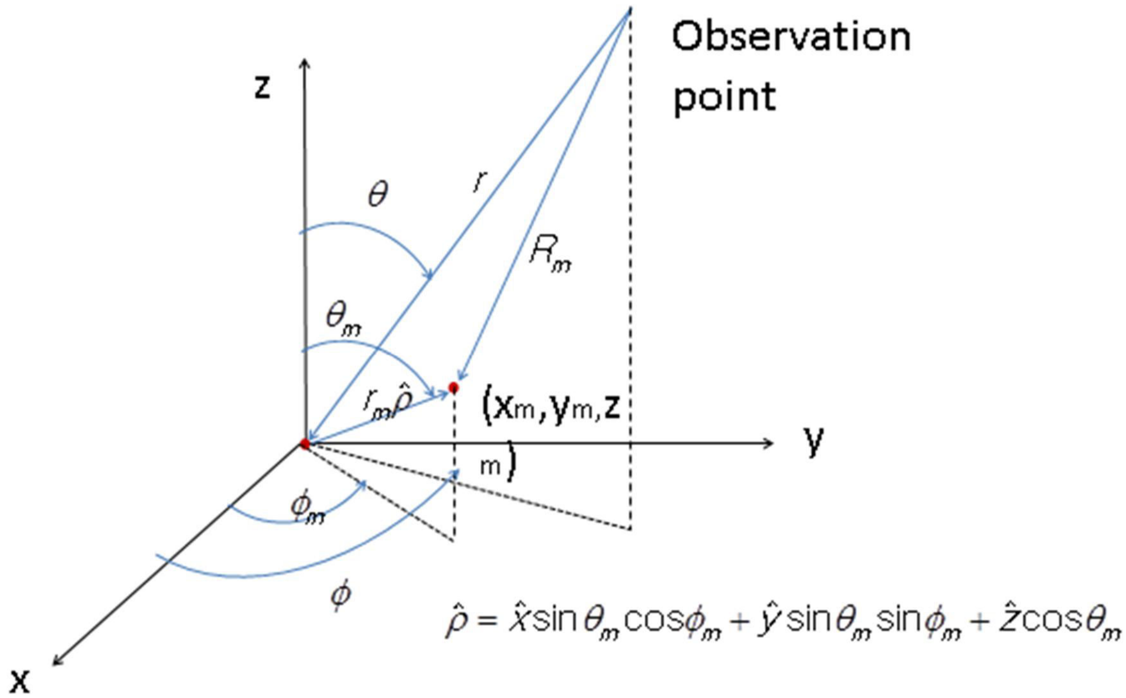

Figure 9: Spherical coordinate system for array analysis.

For the far-field approximation, the position R_m can be derived from equations (1) through (3):

$$R_m = r - r_m(\hat{\rho}\bullet\hat{r}) \tag{1}$$

$$\begin{aligned}\hat{\rho}\bullet\hat{r} &= \sin\theta\sin\theta_m\cos\phi\cos\phi_m + \sin\theta\sin\theta_m\sin\phi\sin\phi_m + \cos\theta\cos\theta_m \\ &= \sin\theta\sin\theta_m\cos(\phi-\phi_m) + \cos\theta\cos\theta_m \\ &= \varphi(\theta,\phi,\theta_m,\phi_m)\end{aligned} \tag{2}$$

$$E(r,\theta,\phi)=\sum_{m=1}^{M}a_m\frac{e^{-jkR_m}}{r}=\frac{e^{-jkr}}{r}\sum_{m=1}^{M}a_n e^{jkr_m\varphi(\theta,\phi,\theta_m,\phi_m)}$$
$$=\frac{e^{-jkr}}{r}\sum_{m=1}^{M}\alpha_m P(\theta,\phi)e^{j[kr_m\varphi(\theta,\phi,\theta_m,\phi_m)+\beta_m]} \quad (3)$$

In equation (3), a_n is the complex weighting, and $\mathrm{P}(\theta,\emptyset)$ is the element pattern. For coherent phase control $(\theta_o,\emptyset_0)$, α_m and β_m can be expressed as equation (4):

$$\alpha_m = 1,\ \beta_m = -kr_m\varphi(\theta_0,\emptyset_0,\theta_m,\emptyset_m) \quad (4)$$

Because a short time delay (STD) chip and a long time delay (LTD) chip are used in the receiving CLAAS antenna, control bits of STD and LTD for coherent phase summation are calculated from equations (5) through (10). The relative delay D_m occurs due to the geometric position of LTD control bit. The LTD control error is defined by the floating control number (6) and the fixed control word (7) by equation (8). The STD floating control number and fixed control word are defined as equations (9) and (10) in the same manner.

$$D_m = r_m\varphi(\theta,\emptyset,\theta_m,\emptyset_m) \quad (5)$$
$$W_{LTD\_float} = \frac{D_{cell}}{cT_{LTD}} \quad (6)$$
$$W_{LTD\_fixed} = floor(W_{LTD_{float}}) \quad (7)$$
$$E_{LTD} = (W_{LTD_{float}} - W_{LTD_{fixed}}) \quad (8)$$

$$W_{STD\_float} = E_{LTD}/(cT_{STD}) \quad (9)$$
$$W_{STD\_fixed} = round(W_{STD_{float}}) \quad (10)$$

The LTD phase delay concept is depicted in Fig. 10.

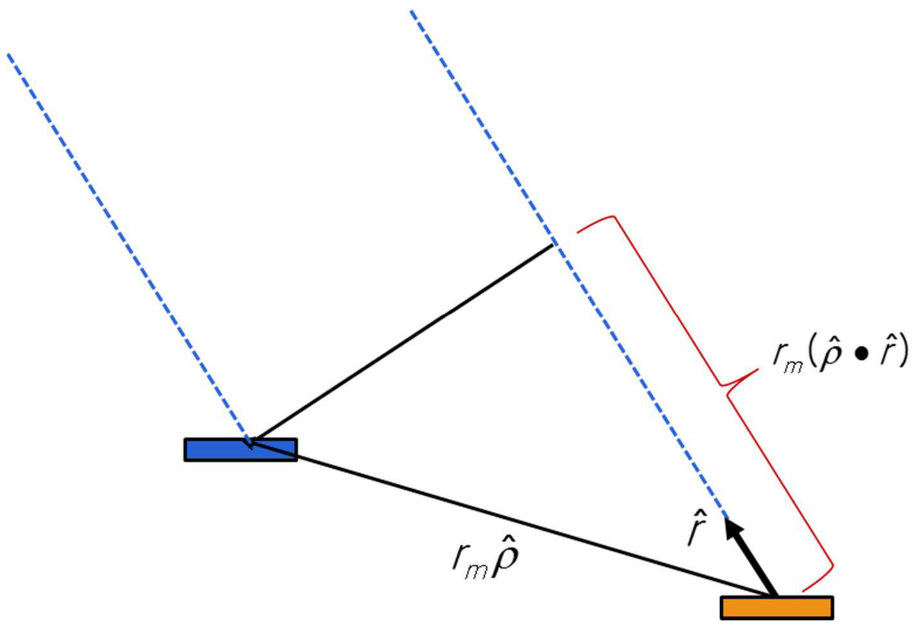

Figure 10: LTD phase delay concept.

3.3 Deflection Effects on CLAAS Antenna Performance

The radiation pattern variation for the Θ=0˚, ϕ=90˚ pointing case at a frequency 12.75 GHz is shown in Fig. 11. The gain reductions for 12.25 GHz and 12.75GHz are shown in Fig. 11(b), and HPBW is 1.5 ˚ to 1.6˚ in Fig. 11(c) when there is no deformation. The radiation pattern variation for Θ=60˚, ϕ=0˚

at 12.75GHz is shown in Fig. 12. A peak gain reduction of 0 dB gain is shown for -60° in Figs. 12(b) and (c), and the HPBW is 3.05° in this case. Fig. 12 shows the case for no deformation of structure.

Antenna performance simulation was conducted using MATLAB code. For the deflected shape of the bottom plate shape, gain reductions are calculated for the beam scanning range ±60° compared with the non-deflected shape. The beam steering ranges of the array antenna system are the elevation angle (θ) from -60° to +60° and the azimuth angle (φ) from 0° to 360°. From Fig. 13, it is seen that the maximum gain value of 0.17 dB is reduced for LC 3 at the position of 0° in the x-direction and at -30° in the y-direction. From Figs. 14 and 15, it is seen that the maximum gain value of 0.17 dB for LC 5 and 1.56 dB for LC 6 is reduced.

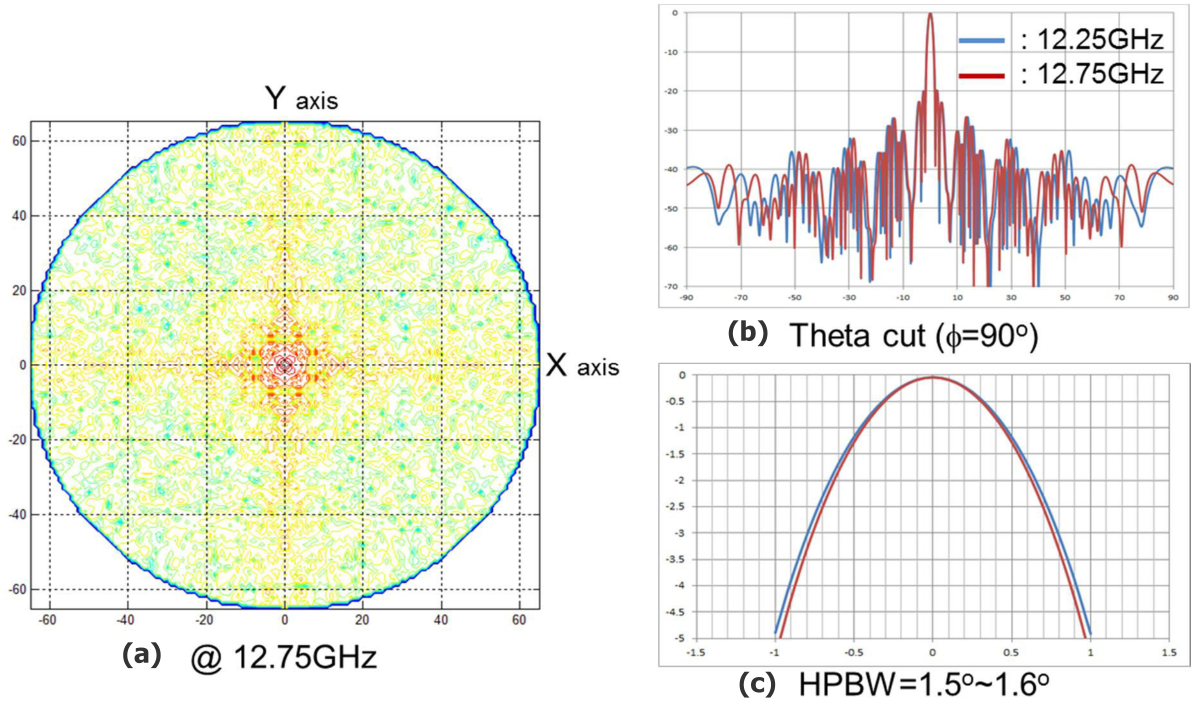

Figure 11: Radiation pattern for theta cut ∅ = 90°.

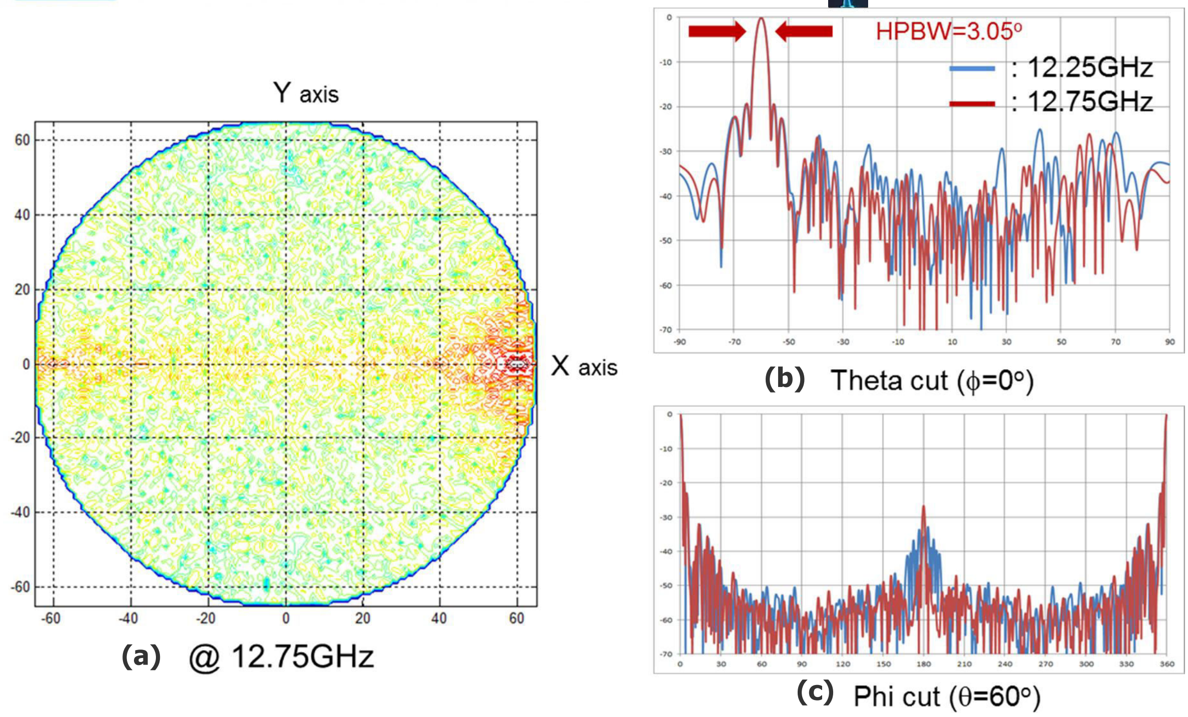

Figure 12: Radiation pattern for theta cut ∅ = 0˚.

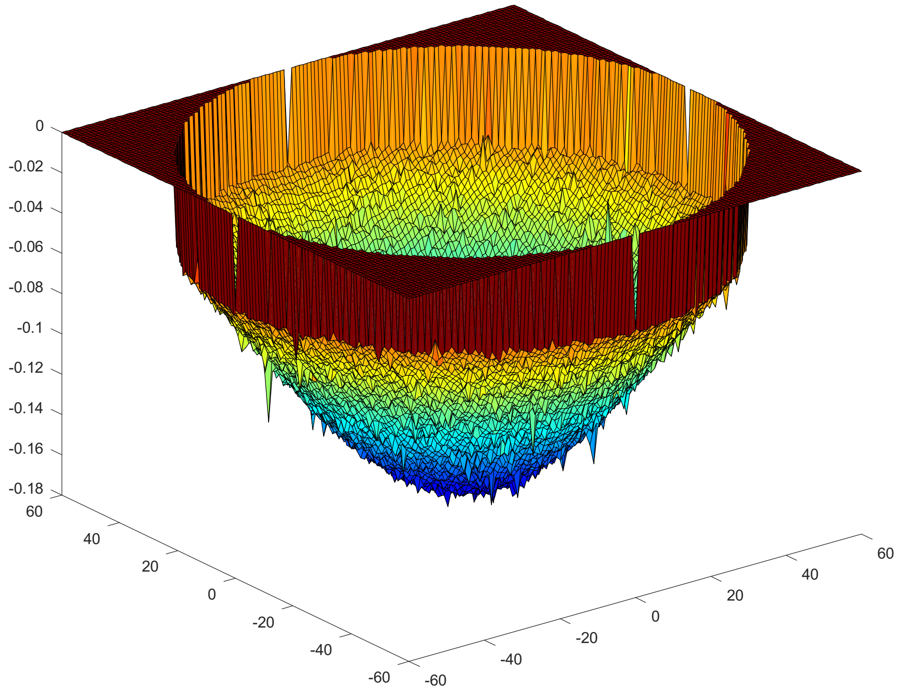

Figure 13: Gain reduction for LC 3.

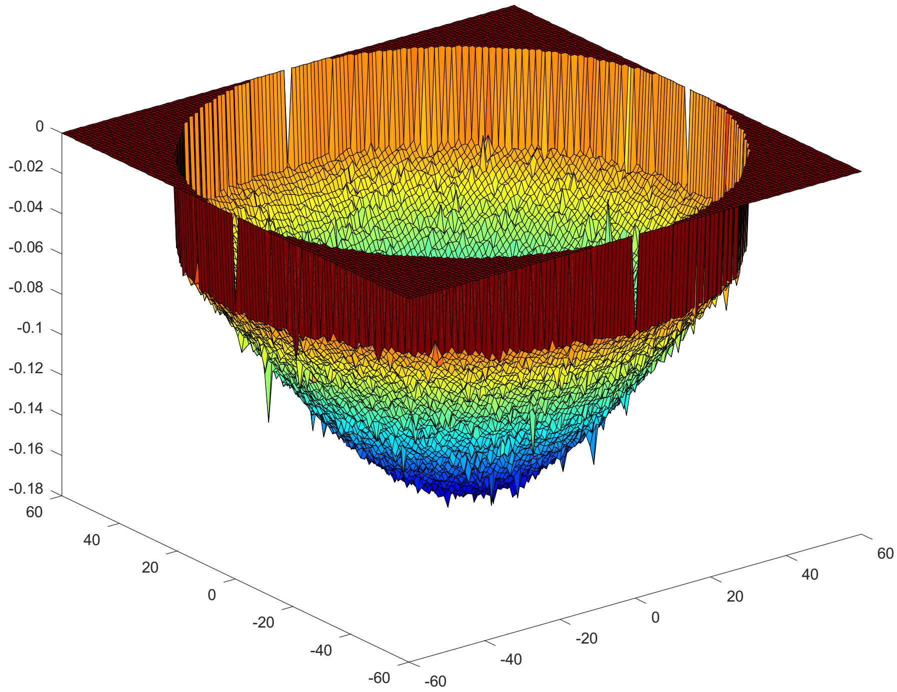

Figure 14: Gain reduction for LC 5.

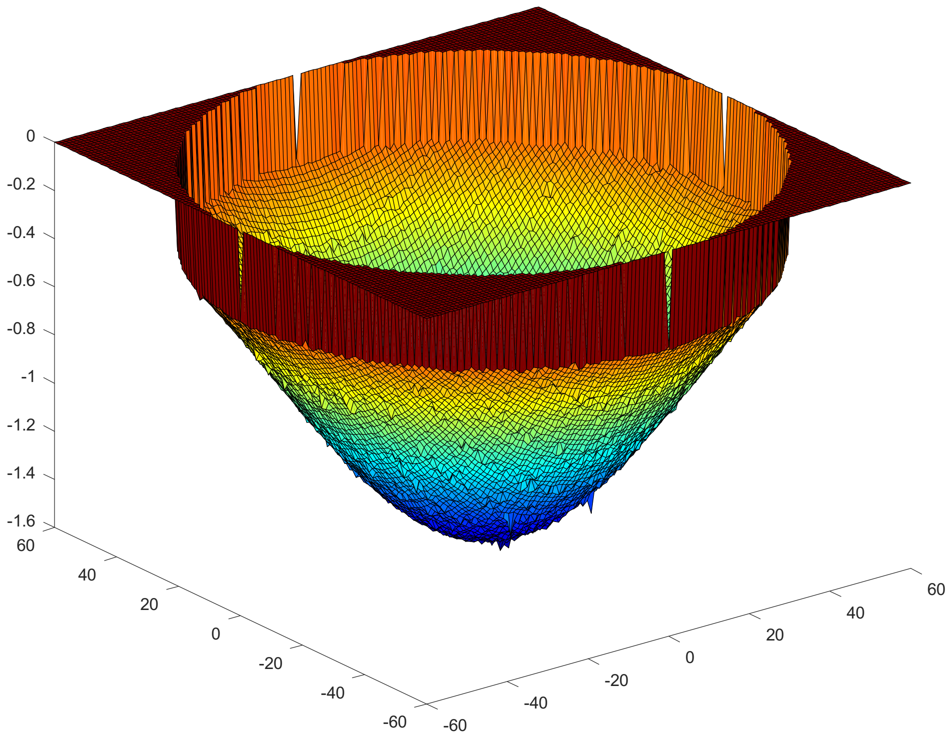

Figure 15: Gain reduction for LC 6.

3.4 Structural Development Test

To verify the structural deformations of the housing plate, a design development test was performed. A housing plate was fabricated as a structural specimen. Structural deformation values for five load conditions were tested. A test rig was designed and fabricated for four load conditions. After installing strain gages and fiber optic sensors, test specimen was fixed on the test setup. Displacement gages were attached to the bottom plate of the housing structure after finishing the test setup. Figs. 16 shows the test setups after attaching all sensors for the four load conditions. The structural test results are compared with the analysis result for test load cases. Table 5 shows the deflection results for the tests and for the analysis. The test result for LC 2 is missing in Table 5 because the test rig for LC 2 was not available. The locations of the strain and fiber optic sensors are the same for all load cases, but the locations of the displacement gages are different for every load cases because the boundary conditions are different for every load case.

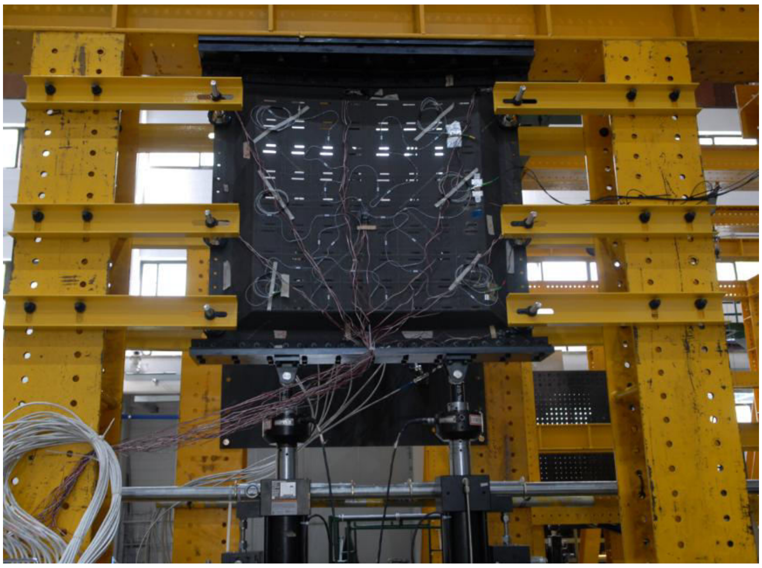

Figure 16: Test setup for LC 1, 2

Table 5. Deformation Result

Load case	Max displacement		Note
	Analysis	Test	
LC1	2.4	2.9	
LC2			No test
LC3	-0.4	-0.4	
LC4	0.3	1.3	
LC5	1.9	4.0	
LC6	-12.5	-10.3	
LC7	12.2	9.9	

4 CONCLUSIONS

This paper deals with the structural deflection effect on the array antenna system in the receiving CLAAS. We found that structural deflection reduces the antenna gain. The Configuration of the deflected shape is considered to find out the gain reduction. The gain reduction results show that the most important factor affecting antenna performance is the maximum deflection length. The other factors affecting antenna performance are found to be the calibration loss, radome loss, assembly loss, alignment loss and beam pointing loss by target tracking error at the moment. The sum of the other factors is assumed to be 2.3 dB. The current antenna gain is 40.5 dBi and the real gain is

derived as 38.2 dBi after considering other factors. The minimum required gain for the receiving CLAAS is 31 dBi. Finally, this paper suggested the allowable deflection length is 1 % of one edge length with a little antenna margin.
This study proposes a new configuration design for the transmitting CLAAS. This study concentrates on the deflection effect of the CLAAS while fulfilling all design requirements. Structural deflection analysis and a structural development test are performed to verify analysis result. MATLAB code is used to predict the antenna performance due to structural deflection. A new design parameter of maximum deflection is suggested for the transmitting CLAAS.

FUNDING

This paper was supported by the Agency for Defense Development's Core-Technology Development Program Fund allocation 2015-5.

REFERENCES

1. U.S. Navy's X-47B Carrier-Capable Stealth UAV Achieved Significant Progress, China Military Report, 2011, http://wuxinghongqi.blogspot.kr/2011/10/us-navys-x-47b-carrier-capable-stealth.html
2. Paul J. Callus; 2007;"Conformal Load-bearing Antenna Structure for Australian Defense Force Aircraft"; *DSTO-TR-1963*; Department of Defense; Australia
3. Allen J. Lockyer, Kevin H. Alt, Jayanth N. Kudva, Jimm Tuss; 2001;"Airvehicle integration issues and considerations for CLAS successful implementation"; *Smart Structures an Materials,* SPIE; June, Vol. 4332; pp. 48 - 59
4. Harmen Schippers, Hans van Tongeren, Jaco Verpoorte and Guus Vos; 2001;"Distortion of conformal antennas on aircraft structures"; *NLR-TP-2001-055*; National Aerospace Laboratory; Netherlands
5. Kim, MS, Park, CY, Cho, CM, et al; 2014; "A multi-band smart skin antenna design for flight demonstration"; *The 8th European Conference on Antennas and Propagation;* April, 6-11; pp. 2855-2859
6. Kim, MS, Park, CY, Jun, SM,; 2012; "Design and experimental validation of a conformal load-bearing antenna structure. Advances in structural Health Management and Composite Structure"; *Advances in Structural Health Management and Composite Structures;* August, 29-31, pp. 49
7. Kim, J, Jang, JY, Ryu, GH, Kim, MS; 2014 ; "Structural design and development of multiband aero-vehicle smart skin antenna"; *Journal of Intelligent Material Systems and Structures;* 25(5); pp. 631-639
8. Baek, SM, Ko, MG, Kim, MS, Joo, YS; 2017; "Structural design of conformal load-bearing array antenna structure(CLAAS)"; *Advanced Composite Materials;* June, 26(S1); pp. 29-42